

CHROMIUM NUCLEOSYNTHESIS AND SILICON-CARBON SHELL MERGERS IN MASSIVE STARS

BENOIT CÔTÉ,^{1,2,3,4} SAMUEL JONES,^{5,4} FALK HERWIG,^{6,3,4} AND MARCO PIGNATARI^{7,1,3,4}

¹*Konkoly Observatory, Research Centre for Astronomy and Earth Sciences, Hungarian Academy of Sciences, Konkoly Thege Miklos ut 15-17, H-1121 Budapest, Hungary*

²*National Superconducting Cyclotron Laboratory, Michigan State University, East Lansing, MI 48824, USA*

³*Joint Institute for Nuclear Astrophysics - Center for the Evolution of the Elements, USA*

⁴*NuGrid Collaboration, <https://nugrid.github.io>*

⁵*X Computational Physics (XCP) Division, Los Alamos National Laboratory, Los Alamos, New Mexico 87545, USA*

⁶*Department of Physics and Astronomy, University of Victoria, Victoria, Canada*

⁷*E.A. Milne Centre for Astrophysics, Department of Physics & Mathematics, University of Hull, HU6 7RX, United Kingdom.*

Submitted to ApJL

ABSTRACT

We analyze the production of the element Cr in galactic chemical evolution (GCE) models using the NuGrid nucleosynthesis yields set. We show that the unusually large [Cr/Fe] abundance at [Fe/H] ≈ 0 reported by previous studies using those yields and predicted by our Milky Way model originates from the merging of convective Si-burning and C-burning shells in a $20 M_{\odot}$ model at metallicity $Z = 0.01$, about an hour before the star explodes. This merger mixes the incomplete burning material in the Si shell, including ^{51}V and ^{52}Cr , out to the edge of the carbon/oxygen (CO) core. The adopted supernova model ejects the outer $2 M_{\odot}$ of the CO core, which includes a significant fraction of the Cr-rich material. When including this $20 M_{\odot}$ model at $Z = 0.01$ in the yields interpolation scheme of our GCE model for stars in between 15 and $25 M_{\odot}$, we overestimate [Cr/Fe] by an order of magnitude at [Fe/H] ≈ 0 relative to observations in the Galactic disk. This raises a number of questions regarding the occurrence of Si-C shell mergers in nature, the accuracy of different simulation approaches, and the impact of such mergers on the pre-supernova structure and explosion dynamics. According to the conditions in this 1D stellar model, the substantial penetration of C-shell material into the Si-shell could launch a convective-reactive global oscillation, if a merger does take place. In any case, GCE provides stringent constraints on the outcome of this stellar evolution phase.

Keywords: Galaxy: abundances - Stars: abundances - Stars: massive - Physical Data and Processes: nuclear reactions, nucleosynthesis, abundances

arXiv:1906.07218v1 [astro-ph.SR] 17 Jun 2019

1. INTRODUCTION

Galactic chemical evolution (GCE) models and simulations are powerful tools to bridge nuclear astrophysics with astronomical observations (e.g., Tinsley 1980; Gibson et al. 2003; Matteucci 2014; Nomoto et al. 2013; Prantzos et al. 2018). In spite of the complexity associated with simulating the formation and evolution of galaxies (e.g., Wise et al. 2012; Schaye et al. 2015; Somerville & Davé 2015; Hopkins et al. 2018; Pillepich et al. 2018; Revaz & Jablonka 2018), the fundamental input ingredients of all GCE studies are still the stellar yields (e.g., Romano et al. 2010; Mollá et al. 2015; Philcox et al. 2018). In the past years, we have developed an open-source galactic chemical evolution (GCE) pipeline in order to bring nuclear astrophysics efforts to the forefront of GCE studies.

There are several sources of uncertainties in generating grids of stellar models for GCE applications, including, for example, uncertainties in nuclear reaction rates (e.g., Lugaro et al. 2004; Tur et al. 2009; Travaglio et al. 2014; deBoer et al. 2017; Nishimura et al. 2017; Denissenkov et al. 2018; Fields et al. 2018), stellar evolution and internal mixing (e.g., Meakin & Arnett 2007; Sukhbold & Woosley 2014; Jones et al. 2015; Davis et al. 2019), and supernova explosion modeling (e.g., Sukhbold et al. 2016; Fryer et al. 2018; Couch et al. 2019; Ebinger et al. 2019; Müller 2019). Turning this argument around, GCE studies are ideal framework to explore the impact of stellar processes in a broader astronomical context (Côté et al. 2017). In this study, we focus on the impact of shell mergers occurring in NuGrid massive star models (Ritter et al. 2018b) during the pre-supernova evolution phase (see also Rauscher et al. 2002, Mocák et al. 2018, and Yadav et al. 2019).

Ritter et al. (2018a) have shown that oxygen-carbon (O-C) shell mergers could potentially be a relevant site for the production of odd-Z elements and p-process isotopes at galactic scale. Androssy et al. (2018), motivated by this, have studied the 3D hydrodynamical properties of O-C shell mergers. Here we discuss the impact of silicon-carbon (Si-C) shell mergers on the evolution of chromium (Cr) in the Milky Way. Since the publication of the second set of NuGrid yields (Ritter et al. 2018b), an overproduction of Cr at galactic scale has been reported by Herwig et al. (2018) and Philcox et al. (2018) when using these yields in GCE codes. We have isolated the source of this overproduction. In the $20 M_{\odot}$ model at $Z = 0.01$, a Si-C shell merger mixes

large amounts of Cr, synthesized during Si-shell burning, above the assumed mass cut¹.

In Section 2.1 we use our chemical evolution tools to highlight the Cr overproduction that points to the specific stellar model responsible for this overproduction. In the other subsections of Section 2, we present the relevant parts of the stellar model, show the implication of the Si-C shell merger on the pre-supernova structure, and discuss the convective and burning time scales during the merger event. In Section 3, we conclude and raise open questions regarding the occurrence of Si-C shell mergers in nature and in multi-dimensional hydrodynamic simulations.

2. RESULTS

2.1. Galactic Chemical Evolution Model

We use the GCE code **OMEGA+** (Côté et al. 2018) to bring NuGrid yields (Ritter et al. 2018b) into a galactic context. This code is part of the open-source JINAPyCEE python package² and represents a one-zone GCE model surrounded by a large circumgalactic gas reservoir. The input parameters adopted in this study for regulating the star formation efficiency and the galactic inflow and outflow rates are available online³. We use the initial mass function of Kroupa (2001). For Type Ia supernovae we use the yields of Iwamoto et al. (1999) and assume a total number of 10^{-3} Type Ia supernova per unit of stellar mass formed. As shown below, the overproduction of Cr is so strong that the choice of GCE parameters and Type Ia supernova yields is of little importance.

The upper panel of Figure 1 shows the predicted evolution of Cr abundances as a function of $[\text{Fe}/\text{H}]$. Near $[\text{Fe}/\text{H}] = 0$, our predictions (solid line) have a bump that overestimates disk data by almost an order of magnitude. The $20 M_{\odot}$ stellar model at $Z = 0.01$ is at the origin of the Cr bump (see also Figure 7 in Herwig et al. 2018). When removing this stellar model from the yields set, the bump disappears entirely (dashed line in Figure 1). The bottom panel shows a production of V accompanying the production of Cr. This is not surprising, since V and Cr are made efficiently at similar stellar conditions (e.g., Woosley & Weaver 1995). In agreement with the simulations reported here, $[\text{V}/\text{Fe}]$ is typically underestimated in GCE models at all metal-

¹ Anything below the mass cut is locked inside the compact remnant and does not contribute to the ejected yields.

² <https://github.com/becot85/JINAPyCEE>

³ https://github.com/becot85/JINAPyCEE/blob/master/DOC/OMEGA%2B_Milky_Way_model1.ipynb

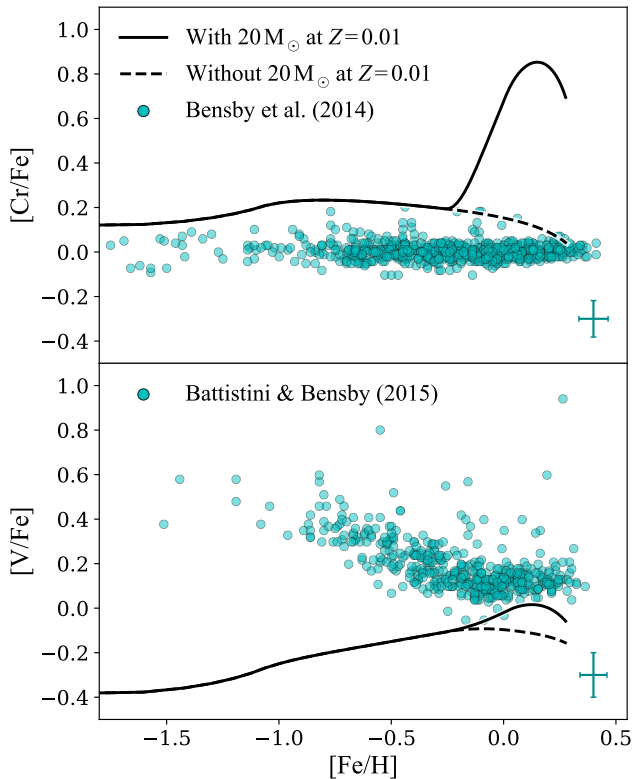


Figure 1. Predicted evolution of $[\text{Cr}/\text{Fe}]$ (top panel) and $[\text{V}/\text{Fe}]$ (bottom panel) as a function of $[\text{Fe}/\text{H}]$ for the Galactic disk using NuGrid yields (Ritter et al. 2018b) and the GCE code OMEGA+ (Côté et al. 2018). The solid and dashed lines show the predictions when including or excluding the $20 M_{\odot}$ model at $Z = 0.01$, respectively. The cyan dots are stellar disk data from Bensby et al. (2014) and Battistini & Bensby (2015).

licities compared to observations (e.g., Prantzos et al. 2018 and references therein).

2.2. Final Evolutionary Stages of the Stellar Model

Here we describe the evolution of the $20 M_{\odot}$ model at $Z = 0.01$. We show that the source of Cr comes from the merging of the C- and Si-burning convective shells during the last hour of evolution before the model collapses.

The Kippenhahn diagrams in Figure 2 show the evolution of convection zones (hatched regions) in the inner $6 M_{\odot}$ of the model. At $t^* \equiv (t_{\text{collapse}} - t)/\text{yr} \approx 10^{-3}$, the convective Si-burning shell engulfs the overlying radiative layer that separated it from the base of the convective C burning shell above. From that time until $t^* \approx 10^{-4}$, the stratified Si- and C-burning convective shells share a convective boundary, which prevents the transport of material from the C shell into the Si shell, and vice versa. Finally, at $t^* \approx 10^{-4}$, the convective boundary is eroded and the Si burning shell extends

from the edge of the Fe core almost to the edge of the CO core. The top panel of Figure 2 shows that ^{52}Cr is mixed out to the edge of the CO core and its mass fraction is slightly reduced owing to dilution by the C shell material.

As shown by our GCE model (Figure 1), a boost of $[\text{Cr}/\text{Fe}]$ is generated above $[\text{Fe}/\text{H}] \approx -0.2$ when the yields of this $20 M_{\odot}$ model are included. One might expect that if the Si-burning shell was mixed out and ejected, then $[\text{Cr}/\text{Fe}]$ should stay relatively flat, since both Cr and Fe are predominant products of Si burning. However, because the Si shell merges while it is still convective, and hence still burning, the ejected chemical signature is typical of incomplete Si burning.

Si burning produces the neutron-magic isotope ^{52}Cr relatively quickly, and thereafter produces ^{56}Fe via a sequence of capture and photodisintegration processes. This is illustrated in Figure 3, which shows the results of a one-zone nuclear reaction network calculation starting from pure ^{28}Si and evolved at density $\rho = 2 \times 10^6 \text{ g cm}^{-3}$ and temperature $T = 2.6 \text{ GK}$, which are approximately the conditions during shell Si burning in the $20 M_{\odot}$ stellar model about an hour before collapse. We note that the time scales of the burning will be different in the star owing to the evolution of the core acting to increase the density and temperature of the shell. However, we have confirmed that the behaviour is similar for a range of temperatures and densities. Only in the most extreme conditions ($10^{10} \text{ g cm}^{-3}$, 5 GK) is Cr produced at the same time as Fe.

The core-collapse supernova (CCSN) explosion for this star was modelled by Ritter et al. (2018b) in the same way as described in Pignatari et al. (2016), with a mass cut at $2.77 M_{\odot}$ based on remnant mass prescription derived in Fryer et al. (2012). In this particular model with these assumptions, a significant fraction of the incomplete Si-shell burning material, including ^{52}Cr and ^{51}V , is ejected during the explosion (the convective Si-C shell extends up to $\sim 2 M_{\odot}$ above the assumed mass cut). The yields from the stellar model are therefore heavily influenced by the occurrence of a Si-C shell merger and by the methods employed to model the supernova.

2.3. Supernova Implications

The $2.77 M_{\odot}$ compact remnant is a black hole created by fallback (Fryer et al. 2012). In agreement with Sukhbold et al. (2016) and Ebinger et al. (2019), stars around $20 M_{\odot}$ are generally found to produce more failed explosions and black holes in 1D simulations than for lower initial masses. However, CCSN theory has far from settled on the precise relationship between progenitor structure and explosion properties (Sukhbold &

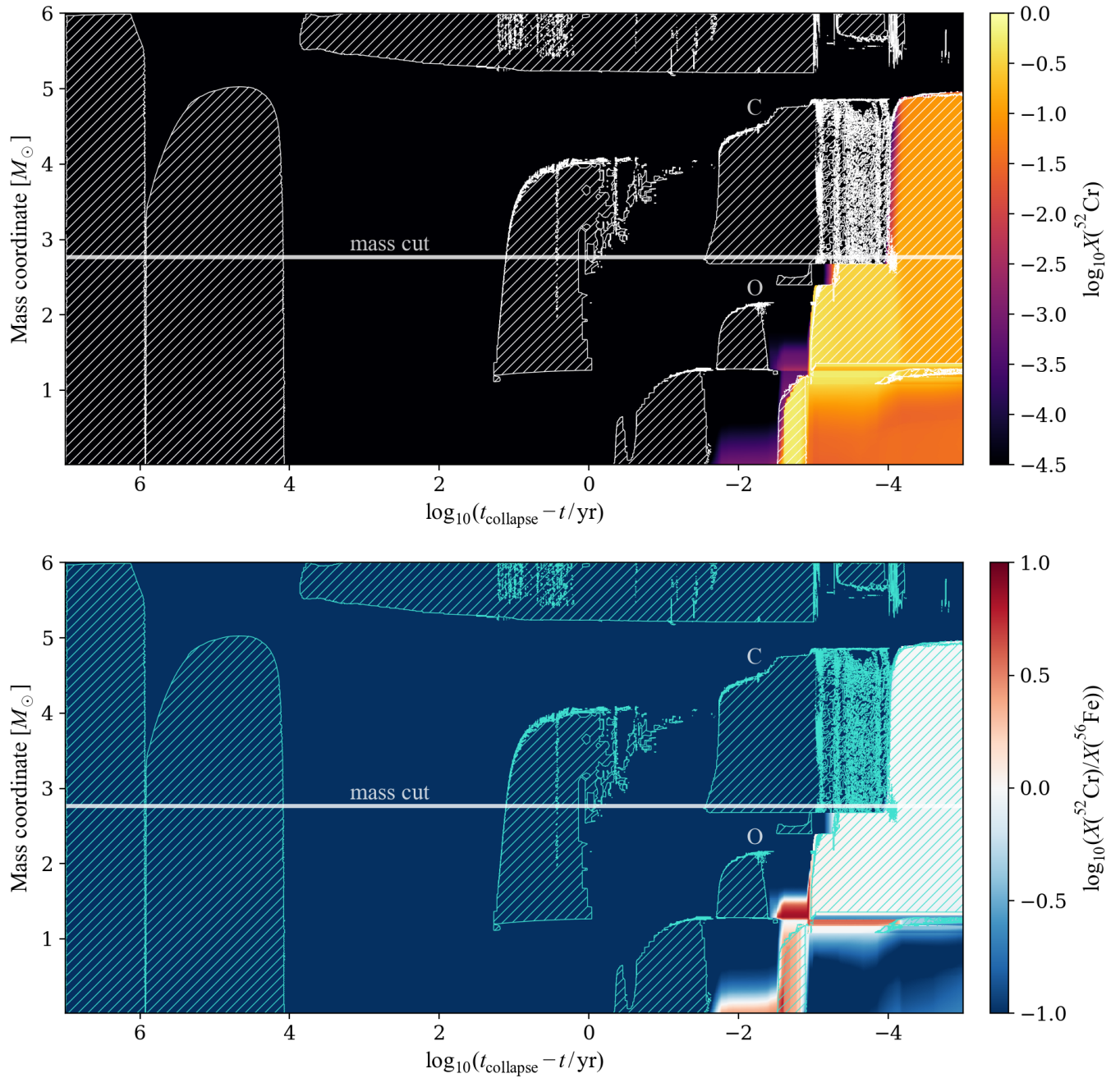


Figure 2. Kippenhahn (convective structure evolution) diagrams of the inner $6 M_{\odot}$ of the $20 M_{\odot}$ model at $Z = 0.01$. The x-axis has an inverse logarithmic time scale showing the time remaining before collapse. Hatched contours show convectively unstable regions and color indicates the mass fraction of ^{52}Cr in the top panel and the $^{52}\text{Cr}/^{56}\text{Fe}$ ratio in the bottom panel. The ratio is approximately unity in the merged C/O/Si shell at the presupernova stage, which is the signature of incomplete Si burning that has been mixed throughout the merged shells. This is the predominant signature that appears in the ejected yields from the stellar model.

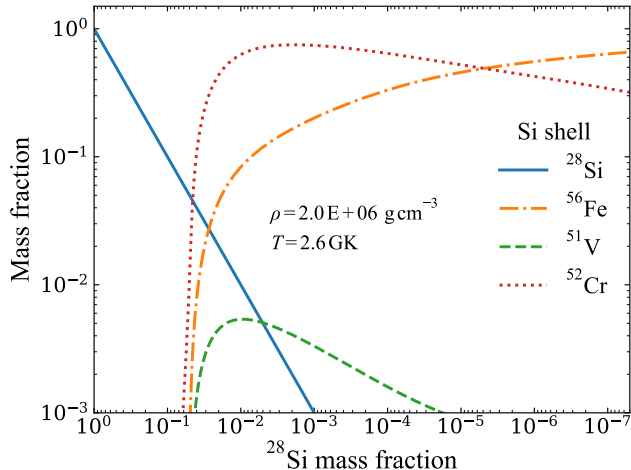


Figure 3. Evolution of key isotopes during a one-zone burn network integration at conditions characteristic of Si shell burning in a $20 M_{\odot}$ star.

Woosley 2014; Müller 2016; Fryer et al. 2018). Even if we did know the remnant mass for a typical model of this initial mass and metallicity, the structure of the core in our model is affected by the shell merger in ways that are likely important in determining the dynamics of the collapse and subsequent explosion, or lack thereof, and compact remnant mass (e.g., Davis et al. 2019; Yadav et al. 2019).

Two of the most important properties of the progenitor models for determining the outcome of the CCSN are the stratification of density and electron fraction (Y_e). The left panel of Figure 4 shows how the Y_e profile is altered by the merger. The right panel shows that the shell merger erases the density jump that existed at the interface of the two shells (see arrow). Such a jump may facilitate the revival of the stalled CCSN shock wave owing to the rapid drop in accretion rate as the shell arrives at the shock radius (Ott et al. 2018). Although this particular density jump appears small, it could still be enough to alleviate the ram pressure at a critical time and allow for a successful explosion. Conversely, it may be that a more realistic simulation of this progenitor model results in direct black hole formation or formation of a much larger black hole than $2.77 M_{\odot}$ by fallback, in which case we would perhaps expect none of the CO core (and hence, none of the Cr) to be ejected. Further implication for the SN explosion may derive from asymmetries that could be seeded right before the explosions in a shell merger, depending on the time scales for convection and burning during the merger.

2.4. Convective Time Scale

The Y_e profile shown in Figure 4 raises another interesting point. The profile is not flat in the newly combined convection zone between 1.4 and $5 M_{\odot}$ (see solid orange line), as revealed by the time-dependent mixing, implemented in the diffusion approximation, when nuclear and mixing time-scales are similar. The pre-supernova profile represents a state of incomplete mixing of the material in the two shells. The convective time scale τ_{conv} , assuming it is approximately the time taken for a fluid element to complete one cycle of advection around a convective cell whose diameter is the shell’s thickness, is given by

$$\tau_{\text{conv}} \approx \frac{2\pi r_{\text{cell}}}{\langle v_{\text{conv}} \rangle} \approx \frac{(7.4 \times 10^9) \pi \text{ cm}}{6.3 \times 10^6 \text{ cm s}^{-1}} = 3690 \text{ s}. \quad (1)$$

The shell merger takes place 10^{-4} yr or 3154 seconds before collapse, which is a similar time scale.

This raises the question of how efficient will be the mixing of ^{52}Cr and other Si-burning products into the outer core if there is only one turnover time to do it. Certainly the use of mixing length theory (MLT) for convection becomes inappropriate under these conditions because MLT only predicts convection properties in terms of averages over many convective turn-over time-scales.

2.5. Burning Time Scale During Shell Merger

The constitution of the C shell should burn rapidly when exposed to the temperatures in the Si-burning shell. This energetic feedback will likely modify the flow dynamics and it should be considered when modeling the pre-supernova evolution of such a star (e.g. Herwig et al. 2014; Androssy et al. 2018; Yadav et al. 2019).

We have estimated the burning time scale of ^{12}C by performing a simple nuclear network calculation beginning from 90% ^{28}Si and 10% ^{12}C . We keep the temperature fixed at 3 GK and the density at $1.4 \times 10^8 \text{ g cm}^{-3}$. We define the burning time scale as the e-folding time of the ^{12}C mass fraction X_C under such conditions,

$$\tau_{\text{burn}} \approx \frac{dt}{d \ln X_C}. \quad (2)$$

For example, near the bottom of the Si shell the time scale is $\sim 10^{-3}$ s, which is much shorter than the $\sim 10^3$ s convective time scale, giving an exceptionally large Damköhler number of $\text{Da} = \tau_{\text{mix}}/\tau_{\text{burn}} \approx 10^6$ (Figure 5). This means the material in the C shell will never actually reach the bottom of the convection zone. Instead, the situation is reminiscent of the H-ingestion into He-shell convection in a post-AGB star. The distributed combustion flame is located where $\text{Da} \sim 1$ (Herwig et al. 2011), which in this case is in the lower third of the Si

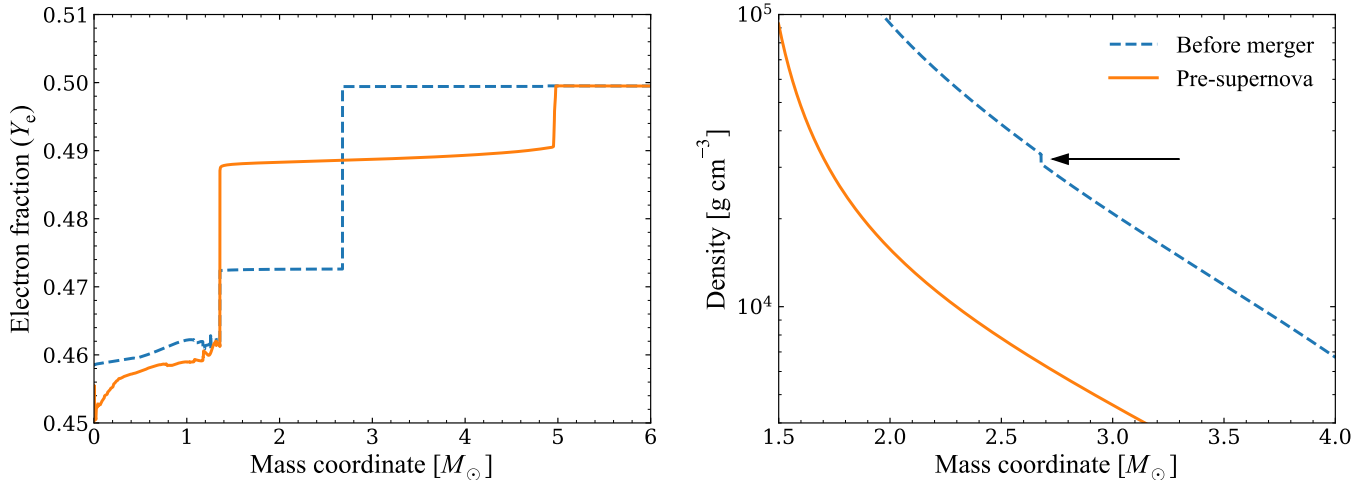


Figure 4. Electron fraction profile (left panel) and density profile (right panel) in the core of the stellar model before the shell merger and at the pre-supernova stage.

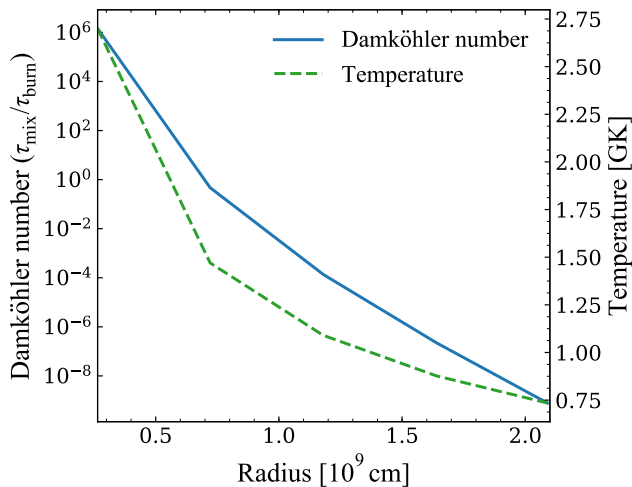


Figure 5. Damköhler number (blue solid line) and temperature (green dashed line) as a function of radius within the Si shell, about 20 cycles before the Si-C shell merger. The range of radius shown represents the boundaries of the convective Si shell.

convection zone. Depending on the energy release of the convective-reactive burn relative to the initial convective kinetic energy, a global non-spherical convective-reactive instability may ensue, such as the Global Oscillation of Shell H-ingestion (GOSH) that has been reported for H-ingestion into He-shell flash convection (Herwig et al. 2014). The exact nature of the convective-reactive event and its impact on yields requires a more comprehensive 3D hydrodynamics and nucleosynthesis simulation approach which is beyond the scope of this work.

3. CONCLUSIONS

In this paper, we analyzed the Si-C shell merger occurring in the $20 M_\odot$ model at $Z = 0.01$ of the Nu-

Grid collaboration (Ritter et al. 2018b). The Si-C shell merger occurs roughly an hour before collapse. Following this event, a large amount of incomplete Si-burning material, including ^{51}V and ^{52}Cr , is mixed all the way from the Si core to a mass coordinate of $5 M_\odot$, which represents the upper boundary of the C shell as it was before the merger event. The convective time scale of this mixed shell is similar to the delay before the star collapses. As a first order approximation, it is therefore possible for the incomplete Si-burning material to mix and fill the Si-C shell by the time of the explosion. Because the adopted mass cut for this model is $2.77 M_\odot$, a significant fraction of Cr is ejected during the explosion.

Using our GCE code OMEGA+ (Côté et al. 2018), and assuming that the ejecta of this specific $20 M_\odot$ model at $Z = 0.01$ is representative of all $20 M_\odot$ stars at that metallicity, we overestimate the predicted evolution of $[\text{Cr}/\text{Fe}]$ in the Milky Way by almost an order of magnitude at $[\text{Fe}/\text{H}] \sim 0$. A question that emerges is whether or not Si-C shell mergers occur in nature. From this experiment, the only conclusion we can draw from a GCE perspective is that the specific conditions (assumptions), in which this $20 M_\odot$ model evolves and explodes, cannot be representative of all $20 M_\odot$ stars and should be extremely rare if they occur at all.

From the analysis of the stellar evolution model, the Si-C merger could launch a non-spherical, global, convective-reactive instability similar to the GOSH found in H-ingestion in post-AGB stars (Herwig et al. 2014). Such an instability could seed substantial non-spherical perturbations of the initial conditions for the SN explosion. Another implication could be that such an instability enhances mixing of Cr-rich Si-shell material into the C-shell above. This would impact the

amount of Cr ejected in this model. If such instabilities occur, their properties will depend on the detailed balance between energy produced from the entrainment of C-shell material and the driving energetics of the Si-burning convection shell. Without such instability, if no or only a partial merger would take place, the convective mixing time scale in the C-shell is similar to the remaining time to collapse, and dredge-up of Cr into the C-shell convection zone would likely be incomplete.

3D hydrodynamic simulations are required to investigate the range of mixing and burning conditions during interactions between the Si and C shells. Such an investigation would address important questions. How would a Si-C shell merger look in multi-dimensional hydrodynamic simulations? To what extent would Cr make its way up into the C shell? How would an interaction between the Si and C shells impact the pre-supernova structure and the dynamics of the supernova explosion? Would the star explode? In any case, GCE would provide stringent constraints on the frequency and efficiency of Cr production through this process, which this study shows must remain small.

This research is supported by the ERC Consolidator Grant (Hungary) funding scheme (Project RADIOSTAR, G.A. n. 724560), by the National Science Foundation (NSF, USA) under grant No. PHY-1430152 (JINA Center for the Evolution of the Elements), and by the US Department of Energy LDRD program through the Los Alamos National Laboratory. Los Alamos National Laboratory is operated by Triad National Security, LLC, for the National Nuclear Security Administration of U.S. Department of Energy (Contract No. 89233218NCA000001). MP acknowledges significant support to NuGrid from STFC (through the University of Hull's Consolidated Grant ST/R000840/1), and access to VIPER, the University of Hull High Performance Computing Facility. MP acknowledges the support from the "Lendulet-2014" Programme of the Hungarian Academy of Sciences (Hungary).

REFERENCES

- Andrassy, R., Herwig, F., Woodward, P., & Ritter, C. 2018, arXiv e-prints, arXiv:1808.04014 [astro-ph.SR]
- Battistini, C., & Bensby, T. 2015, *A&A*, 577, A9
- Bensby, T., Feltzing, S., & Oey, M. S. 2014, *A&A*, 562, A71
- Côté, B., O'Shea, B. W., Ritter, C., Herwig, F., & Venn, K. A. 2017, *ApJ*, 835, 128
- Côté, B., Silvia, D. W., O'Shea, B. W., Smith, B., & Wise, J. H. 2018, *ApJ*, 859, 67
- Couch, S. M., Warren, M. L., & O'Connor, E. P. 2019, arXiv e-prints, arXiv:1902.01340 [astro-ph.HE]
- Davis, A., Jones, S., & Herwig, F. 2019, *MNRAS*, 484, 3921
- deBoer, R. J., Görres, J., Wiescher, M., et al. 2017, *Reviews of Modern Physics*, 89, 035007
- Denissenkov, P., Perdikakis, G., Herwig, F., et al. 2018, *Journal of Physics G Nuclear Physics*, 45, 055203
- Ebinger, K., Curtis, S., Fröhlich, C., et al. 2019, *ApJ*, 870, 1
- Fields, C. E., Timmes, F. X., Farmer, R., et al. 2018, *ApJS*, 234, 19
- Fryer, C. L., Andrews, S., Even, W., Heger, A., & Safi-Harb, S. 2018, *ApJ*, 856, 63
- Fryer, C. L., Belczynski, K., Wiktorowicz, G., et al. 2012, *ApJ*, 749, 91
- Gibson, B. K., Fenner, Y., Renda, A., Kawata, D., & Lee, H.-c. 2003, *PASA*, 20, 401
- Herwig, F., Pignatari, M., Woodward, P. R., et al. 2011, *ApJ*, 727, 89
- Herwig, F., Woodward, P. R., Lin, P.-H., Knox, M., & Fryer, C. 2014, *ApJL*, 792, L3
- Herwig, F., Andrassy, R., Annau, N., et al. 2018, *ApJS*, 236, 2
- Hopkins, P. F., Wetzell, A., Kereš, D., et al. 2018, *MNRAS*, 480, 800
- Iwamoto, K., Brachwitz, F., Nomoto, K., et al. 1999, *ApJS*, 125, 439
- Jones, S., Hirschi, R., Pignatari, M., et al. 2015, *MNRAS*, 447, 3115
- Kroupa, P. 2001, *MNRAS*, 322, 231
- Lugaro, M., Ugalde, C., Karakas, A. I., et al. 2004, *ApJ*, 615, 934
- Matteucci, F. 2014, *The Origin of the Galaxy and Local Group*, Saas-Fee Advanced Course, Volume 37. ISBN 978-3-642-41719-1. Springer-Verlag Berlin Heidelberg, 2014, p. 145, 37, 145
- Meakin, C. A., & Arnett, D. 2007, *ApJ*, 667, 448
- Mocák, M., Meakin, C., Campbell, S. W., & Arnett, W. D. 2018, *MNRAS*, 481, 2918
- Mollá, M., Cavichia, O., Gavilán, M., & Gibson, B. K. 2015, *MNRAS*, 451, 3693
- Müller, B. 2016, *PASA*, 33, e048
- . 2019, arXiv e-prints, arXiv:1902.04270 [astro-ph.SR]
- Nishimura, N., Hirschi, R., Rauscher, T., St. J. Murphy, A., & Cescutti, G. 2017, *MNRAS*, 469, 1752

- Nomoto, K., Kobayashi, C., & Tominaga, N. 2013, *ARA&A*, 51, 457
- Ott, C. D., Roberts, L. F., da Silva Schneider, A., et al. 2018, *ApJ*, 855, L3
- Philcox, O., Rybizki, J., & Gutcke, T. A. 2018, *ApJ*, 861, 40
- Pignatari, M., Herwig, F., Hirschi, R., et al. 2016, *ApJS*, 225, 24
- Pillepich, A., Springel, V., Nelson, D., et al. 2018, *MNRAS*, 473, 4077
- Prantzos, N., Abia, C., Limongi, M., Chieffi, A., & Cristallo, S. 2018, *MNRAS*, 476, 3432
- Rauscher, T., Heger, A., Hoffman, R. D., & Woosley, S. E. 2002, *ApJ*, 576, 323
- Revaz, Y., & Jablonka, P. 2018, *A&A*, 616, A96
- Ritter, C., Andrassy, R., Côté, B., et al. 2018a, *MNRAS*, 474, L1
- Ritter, C., Herwig, F., Jones, S., et al. 2018b, *MNRAS*, 480, 538
- Romano, D., Karakas, A. I., Tosi, M., & Matteucci, F. 2010, *A&A*, 522, A32
- Schaye, J., Crain, R. A., Bower, R. G., et al. 2015, *MNRAS*, 446, 521
- Somerville, R. S., & Davé, R. 2015, *ARA&A*, 53, 51
- Sukhbold, T., Ertl, T., Woosley, S. E., Brown, J. M., & Janka, H.-T. 2016, *ApJ*, 821, 38
- Sukhbold, T., & Woosley, S. E. 2014, *ApJ*, 783, 10
- Tinsley, B. M. 1980, *FCPh*, 5, 287
- Travaglio, C., Gallino, R., Rauscher, T., et al. 2014, *ApJ*, 795, 141
- Tur, C., Heger, A., & Austin, S. M. 2009, *ApJ*, 702, 1068
- Wise, J. H., Turk, M. J., Norman, M. L., & Abel, T. 2012, *ApJ*, 745, 50
- Woosley, S. E., & Weaver, T. A. 1995, *ApJS*, 101, 181
- Yadav, N., Müller, B., Janka, H. T., Melson, T., & Heger, A. 2019, *arXiv e-prints*, arXiv:1905.04378